J Ther Eng, Vol. 10, No. 5, pp. 1137−1148, September, 2024

Journal of Thermal Engineering
Web page info: https://jten.yildiz.edu.tr
DOI: 10.14744/thermal.0000856

Research Article

Heat transfer characteristics of magnetohydrodynamic Casson stratified hybrid nanofluid flow past a porous stretching cylinder

Jintu Mani NATH[1,2,*], Ashish PAUL[1], Tusar Kanti DAS[1,3]

[1]*Department of Mathematics, Cotton University, Guwahati, Assam, 781001, India*
[2]*Department of Mathematics, Mangaldai College, Mangaldai, Assam, 784125, India*
[3]*Department of Mathematics, Dudhnoi College, Dudhnoi, Assam, 783124, India*

ARTICLE INFO

Article history
Received: 17 December 2023
Revised: 16 March 2024
Accepted: 09 April 2024

Keywords:
Casson Hybrid-nanofluid; Heat Source/Sink; Porous Space; Thermal Stratification; Vertical Cylinder

ABSTRACT

In the existence of a thermal source, this study examines the impacts of thermal stratification on the heat transmission characteristics of magnetohydrodynamic water-based copper/molybdenum disulfide Casson hybrid nanofluid flow across a vertical cylinder which is linearly stretching. A magnetic field with an inclination is applied along the stretched vertical cylinder. The driving forces for the flow are due to the stretched cylinder and natural convection. With appropriate similarity transformations, non-linear ordinary differential equations are obtained from the collection of mathematically modeled partial differential equations. The numerical findings are obtained by utilizing the MATLAB bvp4c approach. The consequence of protuberant factors on the thermal and velocity curves is also studied and is depicted pictorially. The outcomes of the friction drag and the thermal transmission rate are summarized in the table. The important contributions highlight that water-based copper/molybdenum disulfide Casson hybrid nanofluids have superior thermal conductivity than water-based copper Casson nanofluids. The water-based Casson hybrid nanofluid fluid has a noteworthy influence on enhancing thermal procedures. Thermal exchangers, solar power systems, automotive cooling down and precision manufacturing are among their beneficial functions. The friction drag for Casson hybrid nanofluid has been found to improve by up to 32.3% when contrasted to water-based Casson nanofluid. While contrasting the Casson hybrid nanofluid with the Casson nanofluid, the thermal transport rate is increased by almost 6.6%. The rate of thermal transmission at the solid surface is negatively impacted by thermal stratification. This finding has practical implications in the areas of bettering materials for thermal insulation and energy-effective designs for buildings. The outcomes reflect a significant enrichment in the discipline of fluid dynamics and nanofluid research since they offer promising potential for heat transfer optimization in various commercial environments.

Cite this article as: Nath JM, Paul A, Das TK. Heat transfer characteristics of magnetohydrodynamic Casson stratified hybrid nanofluid flow past a porous stretching cylinder. J Ther Eng 2024;10(5):1137−1148.

***Corresponding author.**
*E-mail address: nathjintu67@gmail.com

This paper was recommended for publication in revised form by Editor-in-Chief Ahmet Selim Dalkılıç

INTRODUCTION

The most advanced form of nanofluid, termed hybrid nanofluid, can be generated by dispersing two or more distinct types of nanocrystals in the basic fluid. Also, a particular type of nanomaterial that Choi and Eastman [1] first described was incorporated into the common nanofluid. In the past few decades, academics have paid close attention to hybrid nanofluid exploration because it can accelerate thermal transmission compared to conventional nanofluid. Many applications use hybrid nanofluid as their heat exchanger fluid, including cooling equipment for machines, digital equipment, and transformative refrigeration. Devi and Devi [2] focused on the magnetic influence of (Cu - Al_2O_3) nanoparticles to address the transmission of a hybrid nanofluid across the stretched surface. After that, the issue was developed as a 3-dimensional flow problem under Newtonian thermal constraints by Devi and Devi [3]. Both of these investigations demonstrate that, compared to conventional nanofluids, hybrid nanofluids accelerated the heat transition more quickly. Ijaz Khan et al. [4] assessed the hybrid nanofluid's ability to change for heat transmission and pressure loss capabilities due to a higher aspect ratio, a more effective heating system, and the synergistic impacts of nanoparticles. Muneeshwaran et al. [5] provided a brief overview of the hydrothermal characteristics of hybrid nanofluids in diverse thermal transmission applications. Moreover, Sreenivasa et al. [6] computationally analyzed a heat transport mechanism in the hybrid nanofluid movement across an extending cylinder. Also, Yasir et al. [7] comparatively performed an investigation of hybrid nano-particles on radiative flow through a cylinder. Recently, Paul et al. [8] addressed the thermally stratified hybrid nanofluid flow throughout a cylindrical structure, adopting the consequences of an inclined field of magnets and a thermal source/sink. The influence of Hall influences and Cattaneo-Christov thermal flux on the movement of MHD hybrid nanofluid throughout a fluctuating thickness stretched interface was recently addressed by Ali et al. [9]. Furthermore, knowledge concerning significant research endeavors in the field of nanofluids and hybrid nanofluid flow has also been provided by pertinent literature [10] to [19].

The fluid flow through a stretched cylinder has drawn the attention of various researchers. Numerous technological and manufacturing procedures, such as cutting polymer sheets, melting revolving, producing paper, making glass fiber, drawing wire, etc., essentially require the flow through a stretched cylinder. The role of heat radiation and irregular heat flow on Magnetohydrodynamics hybrid nanofluid over a stretching cylinder was addressed by Ali et al. [20]. Furthermore, Khan et al. [21] focused on the radiation mixed-convective flow via a vertical cylinder in a porous region with an imbalanced thermal sink/source. Moreover, Khan et al. [22] explored the radiative thermal transmission of hybrid stagnation point movement over an extending cylinder. Recently, the integrated effect of couple stress, viscosity fluctuation, and magnetohydrodynamics on the squeezing film attributes of a rough flat plate and cylinder was researched by Suresha et al. [23].

Despite its complexity, non-Newtonian fluid mechanics is a research area of exploration because the heat and flow-transmitting attributes of non-Newtonian fluids are vital to various and numerous applications in the fields of bio-technology, medicine, and chemical engineering. The non-Newtonian concept has a non-linear connection between the stress and the strain rate in a broad sense. Conventional approaches may not adequately describe the mechanical features of non-Newtonian fluids, such as shear stress, regular stress differential, and visco-elastic reactivity, accordingly an innovative and accurate description is essential. Casson modeling has a lot of support in addition to the several constitutive equations that have been put forward to reflect the movement and the thermal transport domain. Casson fluid modeling has a broad range of utilisations in power production, geophysical fluid processes, bio-medical and commercial engineering, and many others. Casson fluid modeling, which was first developed by Casson [24], is the most significant rheological model among the various non-Newtonian models.

Casson hybrid nanofluids present distinctive characteristics stemming from their non-Newtonian nature and the incorporation of nanoparticles. These features encompass heightened thermal conductivity, bolstered stability, and adaptable rheological attributes, rendering them highly promising for a spectrum of industrial contexts necessitating optimized heat transfer mechanisms. Empirical investigations have underscored their efficacy across distinct applications such as thermal exchangers, solar collectors, and cooling systems, substantiating their potential to augment thermal processes significantly. Using magnetic field impact and heat convection boundary constraints, Kamran et al. [25] reported a computational investigation of a Casson nano-fluid across a parallel stretched plate. Ramesh et al. [26] investigated how to improve radiation on hydromagnetic Casson fluid moving via a stretched cylinder incorporating fluid-particle suspension. The movement of a hydro-magnetic Casson nanofluid was addressed by Naqvi et al. [27] in a permeable stretched cylinder employing Newtonian thermal and mass constraints. Ragupathi et al. [28] employed computational techniques to simulate the convective flow of Casson nanofluid over a stretching sheet, incorporating Arrhenius activation energy kinetics and exponential thermal source contributions. Continuous exponentially accelerated vertical porous interfaces were employed to explore the radiative magnetohydrodynamic flow of Casson hybrid-nanofluid by Krishna et al. [29]. Jyothi et al. [30] explored the Casson hybrid nanofluid squeeze movement between parallel surfaces employing a source of heat. After that, the hydromagnetic flow of a Casson nanofluid via a porous stretched cylinder having activation energy was investigated by Zeeshan et al. [31]. By

considering the influences of magnetic dipoles and gyrotactic microbes, Wang et al. [32] computationally simulated the movement of a Casson hybrid nanofluid. Saranya et al. [33] analyzed time-dependent Casson and Carreau fluids transporting both minute particles and gyrotactic microorganisms. Additionally, recent literature contributions [34] to [38] have provided supplementary insights into significant research endeavors within this specific domain.

The importance of heat and solute stratification in the transportation of heat and mass has been well-studied by researchers. Distinctions in liquid density, concentration, or temperature can cause stratification in flow fields. The thermal stratification process is used for saline, lakeside thermo-hydraulics, subsurface reserves, and vibratory fluxes. Ishak et al. [39] adopted the implicit finite difference method for exploring the mixed convection flow through the stably stratified medium. The Lie group transformation technique was used by Mukhopadhyay et al. [40] to evaluate the effect of heat stratification over a permeable vertical stretch sheet. Deka and Paul [41, 42] considered the buoyancy force while analyzing the transient flow in a thermally stratified fluid across a vertical cylinder. Again, Deka and Paul [43], Paul and Deka [44] extended the work by Deka and Paul [41, 42] by considering mass stratification. Also, Khashi'ie et al. [45] researched the thermally stratified hybrid nanofluid movement using a circular cylinder. Jafar et al. [46] inspected the Casson nanofluid flow between two spinning discs whenever there is a magnetic field and heat stratification. Incorporating the impact of double stratification, Ahmad et al. [47] evaluated the thermal and mass transmission attributes of Casson hybrid nanofluid flow through a cylinder. Also, Alkasasbeh [48] computationally investigated the thermal transmission movement of hybrid Casson nanofluid via a vertical stretching sheet. The latest study by Paul et al. [49] addressed the Casson hybrid nanofluid movement through an exponentially extending cylinder.

This study delves into the relatively unexplored realm of non-Newtonian fluid dynamics, focusing on Cu - MoS_2/Water Casson hybrid nanofluid flow across a vertical cylinder subjected to free convection and heat stratification, while also considering the consequence of an angled magnetic field. This investigation stands out for its unique combination of factors, namely the joint influence of thermal stratification and free convection on the flow of Cu - MoS_2/water Casson hybrid nanofluid over a linearly stretching cylinder, a phenomenon not previously documented in the literature. So, the research on this phenomenon has a vast scope in the domain of fluid dynamics. The primary novelty is to analyze how the thermal transport rate is affected by the modification of Cu - H_2O Casson nanofluid to Cu - MoS_2/Water Casson hybrid nanofluid in the existence of a heat source. This research is motivated by the intention to strengthen our understanding of the mechanisms behind heat transport acceleration in non-Newtonian fluids. The aim of this investigation is to contribute to the understanding of the intricate interplay between various factors influencing the fluid flow and heat transfer in non-Newtonian fluids, particularly in the context of practical applications involving thermal transfer enhancement. From a practical standpoint, this finding is intriguing in several areas, notably producing goods, thermal engineering, and generating energy, where efficient thermal movement is necessary. Comprehending the impact of nanofluid composition on heating rates can facilitate the creation of enhanced thermal transmission fluids and systems, hence augmenting the efficacy and efficiency of thermal management procedures in these sectors. By adopting the MATLAB-based bvp4c method [50], the numerical simulation of the current analysis is integrated. The various physical factors which govern the steady flow are demonstrated in graphs, and the skin drag and the rate of thermo transport are listed in tables.

MATHEMATICAL MODEL

Let us consider a two-dimensional, steady Casson hybrid nanofluid past across a linearly stretching permeable vertical cylinder in the existence of a heat source/sink. Figure 1 illustrates a schematic overview and coordinate system of the mathematical model.

In the formulation of the mathematical flow model, the subsequent assumptions are postulated.

- The cylindrical polar (x, r) coordinate system used in this flow analysis, in where x and r signify along the axial and radial direction respectively.
- The magnetic field having strength B_0 is employed at an inclination, ξ to the vertical direction.
- With surface velocity, $u_w = a\left(\frac{x}{l}\right)$, along its axis, the cylinder is stretched linearly, in which a and l denote the flow speed and the cylinder's distinctive length.
- $T_w(x) = T_0 + A\left(\frac{x}{l}\right)$ is considered to be wall temperature and $T_\infty(x) = T_0 + B\left(\frac{x}{l}\right)$ is the ambient hybrid nanofluid's temperature. In which A, B and T_0 denote positive constants ($A > B$) and starting temperature, respectively.

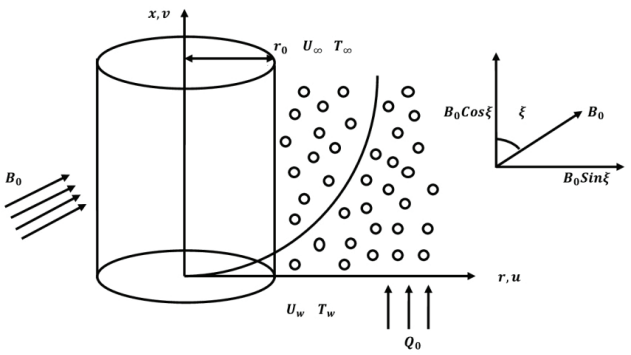

Figure 1. Flow diagram of the model.

· The thermal buoyancy impact is also considered in the momentum equation.

With these flow constraints, the equations of the flow for Casson hybrid nanofluid take the form [8, 45]:

$$\frac{\partial(ru)}{\partial x}+\frac{\partial(rv)}{\partial r}=0 \tag{1}$$

$$u\frac{\partial u}{\partial x}+v\frac{\partial u}{\partial r}=\left(1+\frac{1}{\beta}\right)\frac{\mu_{hnf}}{\rho_{hnf}}\frac{1}{r}\frac{\partial}{\partial r}\left(r\frac{\partial u}{\partial r}\right)+\frac{(\rho\beta)_{hnf}}{\rho_{hnf}}g(T-T_\infty) -\frac{\sigma_{hnf}}{\rho_{hnf}}{B_0}^2.Sin^2\xi.u-\left(1+\frac{1}{\beta}\right)\frac{\mu_{hnf}}{\rho_{hnf}}\frac{u}{k} \tag{2}$$

$$u\frac{\partial T}{\partial x}+v\frac{\partial T}{\partial r}=\frac{k_{hnf}}{(\rho c_p)_{hnf}}\frac{1}{r}\frac{\partial}{\partial r}\left(r\frac{\partial T}{\partial r}\right)+\frac{Q_0}{(\rho c_p)_{hnf}}(T-T_\infty) \tag{3}$$

The boundary limitations are:

$$u=a\frac{x}{l},\ \ v=0,\ \ T=T_w(x)\quad when\ r=r_0$$
$$u=0,\quad T\to T_\infty(x)\qquad when\ r\to\infty \tag{4}$$

The following variables can be used for similarity transformations [51]:

$$\eta=\frac{r^2-{r_0}^2}{2r_0}\sqrt{\frac{a}{\upsilon_f l}},\ \psi=\sqrt{\frac{a\upsilon_f}{l}}xr_0f(\eta),\ \theta=\frac{T-T_\infty(x)}{T_w(x)-T_0}$$

Where $u=\frac{1}{r}\frac{\partial\psi}{\partial r},\ \ v=-\frac{1}{r}\frac{\partial\psi}{\partial x}$

Following the aforementioned transformation, the converted dimensionless non-linear equations are:

$$f'^2-f.f''=Q_1\left(1+\frac{1}{\beta}\right)\{2\gamma f''+(1+2\gamma\eta)f'''\}+Q_2.\lambda.\theta -\{Sin^2\xi.Q_3.M+Q_1\left(1+\frac{1}{\beta}\right)P\}f' \tag{5}$$

$$f'(\theta+\delta)-f\theta'=Q_4.\left(\frac{1}{Pr}\right)\{2\gamma\theta'+(2\gamma\eta+1)\theta''\}+Q_5.S.\theta \tag{6}$$

And the converted boundary constraints are as follows:

$$f'(0)=1,\quad f(0)=0$$
$$\theta(0)=1-\delta,\quad f'(\infty)\to 0,\quad \theta(\infty)\to 0 \tag{7}$$

Where

$$Q_1=\frac{\rho_f}{\rho_{hnf}}\frac{\mu_{hnf}}{\mu_f},\ Q_2=\frac{\rho_f}{\rho_{hnf}}\frac{(\rho\beta)_{hnf}}{(\rho\beta)_f},\ Q_3=\frac{\rho_f}{\rho_{hnf}}\frac{\sigma_{hnf}}{\sigma_f},$$
$$Q_4=\frac{k_{hnf}}{k_f}\frac{(\rho c_p)_f}{(\rho c_p)_{hnf}},\ Q_5=\frac{(\rho c_p)_f}{(\rho c_p)_{hnf}}$$

$$M=\frac{{B_0}^2l\sigma_f}{a\rho_f},\ P=\frac{l}{a}\frac{\vartheta_f}{k},\ \gamma=\sqrt{\frac{l\vartheta_f}{a{r_0}^2}},\ \lambda=\frac{Gr_x}{{Re_x}^2},$$
$$\delta=\frac{B}{A},\ S=\frac{Q_0l}{(\rho c_p)_fa},\ Pr=\frac{\vartheta_f(\rho c_p)_f}{k_f}$$

The density ρ_{hnf}, thermal conductivity k_{hnf}, thermal expansion $(\rho\beta_T)_{hnf}$, dynamic viscosity μ_{hnf}, and heat capacity $(\rho C_p)_{hnf}$ of hybrid nanofluid are defined as follows [8, 51]:

$$\rho_{hnf}=(1-\phi_2)\{(1-\phi_1)\rho_f+\phi_1\rho_{s1}\}+\phi_2\rho_{s2},$$

$$k_{hnf}=k_{bf}\left\{\frac{k_{s2}+2k_{bf}-2\phi_2(k_{bf}-k_{s2})}{k_{s2}+2k_{bf}+\phi_2(k_{bf}-k_{s2})}\right\}$$

Where $k_{bf}=k_f\left\{\frac{k_{s1}+2k_f-2\phi_1(k_f-k_{s1})}{k_{s1}+2k_f+\phi_1(k_f-k_{s1})}\right\}$,

$$(\rho\beta_T)_{hnf}=(1-\phi_2)\{(1-\phi_1)(\rho\beta_T)_f+\phi_1(\rho\beta_T)_{s1}\}+\phi_2(\rho\beta_T)_{s2},$$

$$\mu_{hnf}=\frac{\mu_f}{(1-\phi_1)^{2.5}(1-\phi_2)^{2.5}},$$

$$(\rho C_p)_{hnf}=(1-\phi_2)\left\{(1-\phi_1)(\rho C_p)_f+\phi_1(\rho C_p)_{s1}\right\}+\phi_2(\rho C_p)_{s2}$$

The friction drag and the Nusselt number are determined as follows:

$$C_fRe_x{}^{1}/_{2}=\frac{1}{(1-\phi_1)^{2.5}(1-\phi_2)^{2.5}}(1+\frac{1}{\beta})f''(0)$$
$$Nu_xRe_x{}^{-1}/_{2}=-\frac{k_{hnf}}{k_f}\theta'(0)$$

Methodology

The computational tool known as bvp4c is harnessed to computationally elucidate the interlinked higher-order ordinary differential equations (5)–(6), under the constraints specified in equations (7), across a spectrum of distinct values for the physical parameters encompassing the Prandtl number, thermal source/sink index, Magnetic factor, Porosity term, Curvature factor, Thermal stratification factor, Casson factor, Magnetic field Inclination, and Thermal buoyancy term. Employing the Lobatto IIIa formula in its three phases, the MATLAB BVP solver, bvp4c, is utilized, which operates as a finite difference code. Through the utilization of bvp4c within MATLAB, equations (1) to (3) are reformulated into a set of initial value problems represented as first-order equations. The theoretical underpinning of the bvp4c methodology is expounded by Shampine et al. [50]. Consequently, assuming the vector $[y(1)\ y(2)\ y(3)\ y(4)\ y(5)]^T=[f f' f''\ \theta\ \theta']^T$ is established, whereby each component corresponds to specific variables and their derivatives, and the numerical analysis proceeds.

$$\frac{d}{d\eta}\begin{pmatrix} y(1) \\ y(2) \\ y(3) \\ y(4) \\ y(5) \end{pmatrix} = \begin{pmatrix} y(2) \\ y(3) \\ \left(\frac{1}{1+(2*\gamma*\eta)}\right)*\left(\left(\left(\frac{1}{Q_1}\right)*\left(1+\frac{1}{\beta}\right)^{-1}*\left(y(2)^2-y(1)*y(3)-Q_2*\lambda*y(4)+\left(Sin^2\xi*Q_3*M+Q_4*P*\left(1+\frac{1}{\beta}\right)\right)*y(2)\right)\right)-2*\gamma*y(3)\right) \\ y(5) \\ \left(\frac{1}{1+(2*\gamma*\eta)}\right)*\left(\left(\frac{Pr}{Q_4}\right)*\left(y(2)*y(4)+y(2)*\delta-y(1)*y(5)-Q_5*S*y(4)\right)-2*\gamma*y(5)\right) \end{pmatrix}$$

RESULTS AND DISCUSSION

A vertically stretched cylinder is used to investigate the flow of a thermally stratified *Cu* - MoS_2/water Casson hybrid nanofluid through a porous media that also incorporates the heat source effect. In the present flow context, 0.1 volume portion of MoS_2 nanomaterials and 0.05 volume portion of *Cu* nanoparticles are incorporated with water to create a hybrid nanofluid. Throughout every aspect of the analysis, the aforementioned volume proportion remains static. Table 1 [45,52] documents the thermos-physical traits of the base fluid and the hybrid nanocrystals. The computational findings are extracted by computing the non-linear coupled ODEs by employing the Bvp4c algorithm. Graphs and tables are used to show how different dimensionless dynamic parameters, including the heat source factor, the thermal stratification factor, the porosity factor, the Prandtl number, and the Casson factor impacted the thermal and velocity curves, also the rate of thermal transmission and the friction drag.

In Table 2, the outcomes obtained in the current investigation are contrasted with those reported by Elbashbeshy et al. [53] and Paul et al. [51] in the omission of nano-particle volume proportions with $M = \gamma = \delta = S = \lambda = P = 0,\ \xi = \frac{\pi}{2}, \beta \to \infty$ and distinct values of Prandtl number. Contrasting the bvp4c solver's computational outcomes to those of the other methodologies confirms its results are trustworthy and precise.

The Casson fluid parameter β has an impact on the velocity and thermal curve, as shown in Figures 2 and 3. As β enhances, the yield stress and boundary layer thickness

Table 1. Thermo-physical features of base fluid and nano-particles 45,52]

Thermo-physical features	ρ (kg/m^3)	C_p (J/kgK)	k (W/mK)	β_T (K^{-1})
MoS_2	5060	397.21	904.4	2.8424 x 10^{-5}
Cu	8933	385	400	1.67 x 10^{-5}
H_2O	997.1	4179	0.6130	21 x 10^{-5}

Table 2. The comparable findings of $-\theta'(0)$ with $M = P = \gamma = \delta = S = \lambda = \phi_1 = \phi_2 = 0$, $\xi = \pi/2$, $\beta \to \infty$ and various values of Prandtl number

Pr	Elbashbeshy et al. [53]	Paul et al. [51]	Present Study
1	1.0000	1.0005	1.0005
10	3.7207	3.7200	3.7200

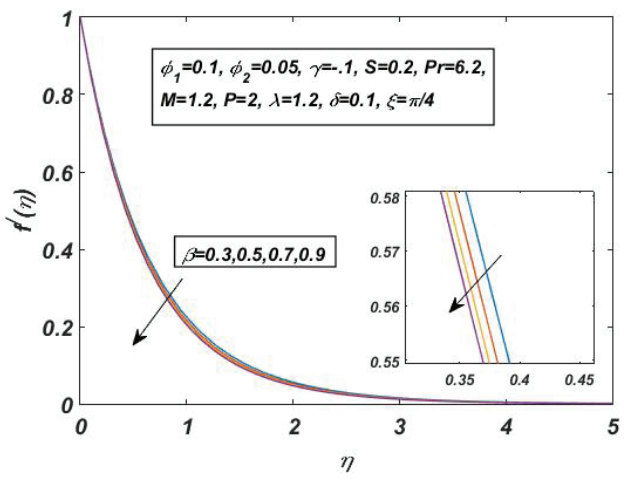

Figure 2. Impact of β on velocity curve.

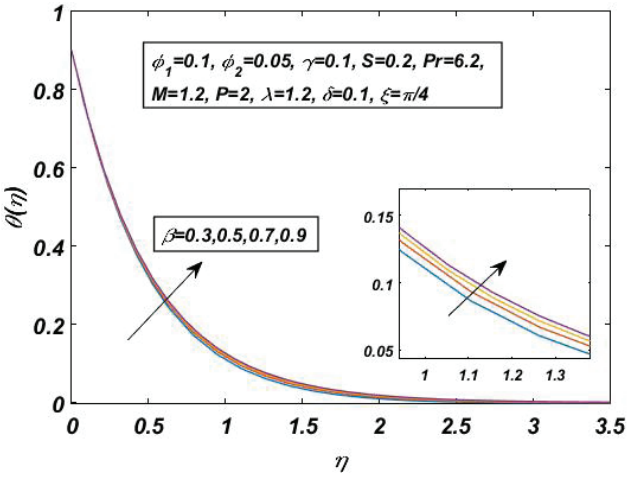

Figure 3. Impact of β on thermal curve.

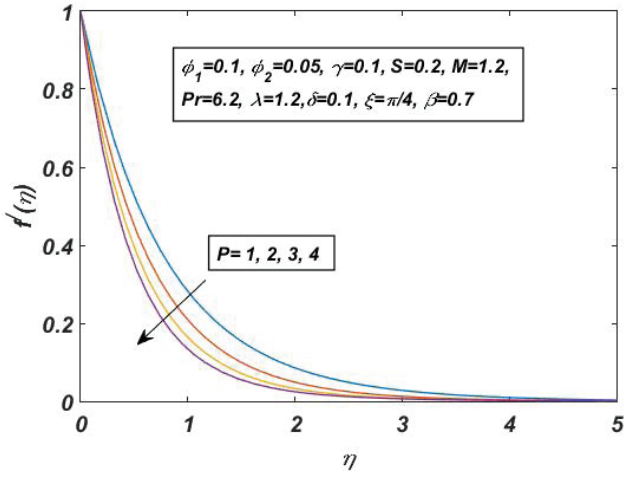

Figure 4. Impact of *P* on velocity curve.

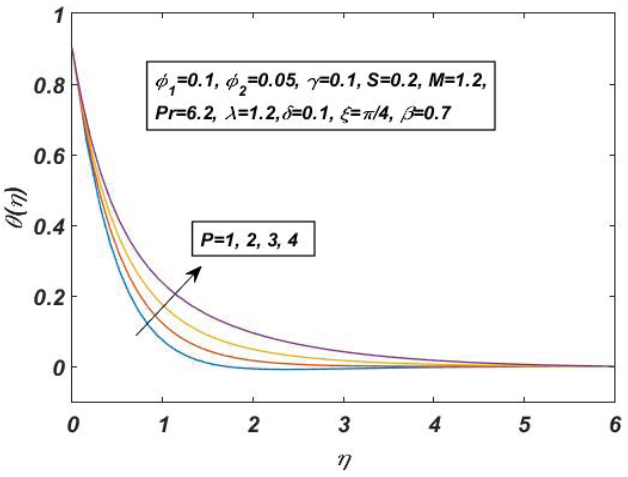

Figure 5. Impact of *P* on thermal curve.

both grow, strengthening the fluid's viscosity. As a consequence, Figure 2 confirms the decline in fluid velocity. However, the temperature curve shown in Figure 3 is boasted with β in the reverse direction. A fluid exhibiting a larger Casson fluid component has an elevated yield stress and demands more energy to overcome the flow resistance. As a consequence, the fluid's heat energy confronts more barriers to flow, which causes thermal energy to accumulate and the thermal profile to elevate. The same outcomes were reported by Naqvi et al. [27] for Casson nanofluid flow through a permeable stretched cylinder. However, this conclusion has been proven for the *Cu - MoS_2*/water Casson hybrid nanofluid over a cylinder that is stretched vertically.

Figures 4 and 5 portrayed how porosity impacted the velocity and thermal curves, respectively. Whenever P elevates, the diameter of the porous region shrinks because of the inverse connection between those two quantities. This makes it difficult for the fluid to move through the porous area. The fluid velocity was decreased as a result of this obstruction brought on by the porosity, while the thermal profile reflected the opposite trend as P improved. Physically, Superior porosity indicates that there are more pathways for the fluid to pass through, boosting the fluid's potential to transmit heat. The void spaces allow for improved fluid mixing and convective thermal transfer, leading to an enhanced heat profile.

Figures 6 and 7, accordingly, highlight how the heat source factor influences the flow speed and the temperature profiles. As the positive magnitudes of the heat source factor, scale higher, both velocity and temperature curves improve. An upsurge in the thermal source factor signifies more energy is being delivered to the mechanism, which elevates the fluid's temperature gradient. Greater buoyancy forces are produced by this higher temperature gradient, which accelerates the fluid and raises its velocity profiles. Also, a stronger thermal profile develops whenever the heat source component improves due to the fluid's thermal mixing being accelerated by the heat energy entering the system.

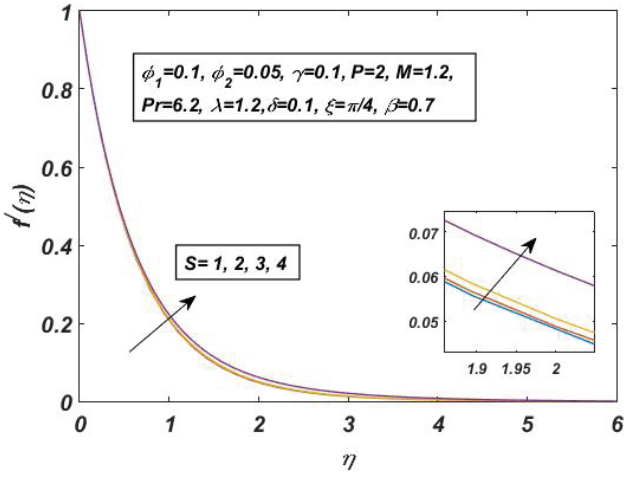

Figure 6. Impact of S on velocity curve.

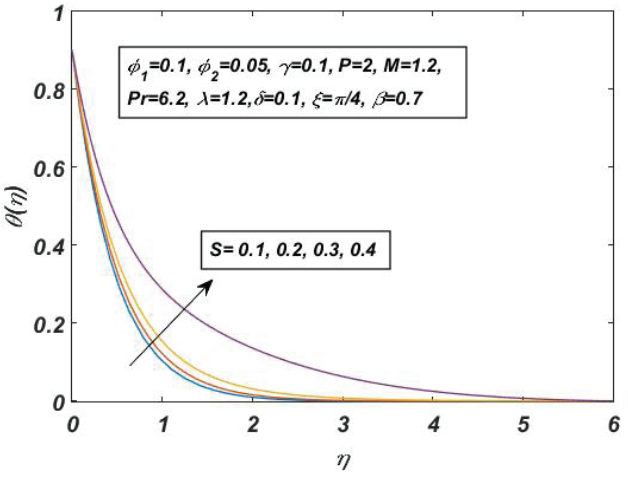

Figure 7. Impact of S on thermal curve.

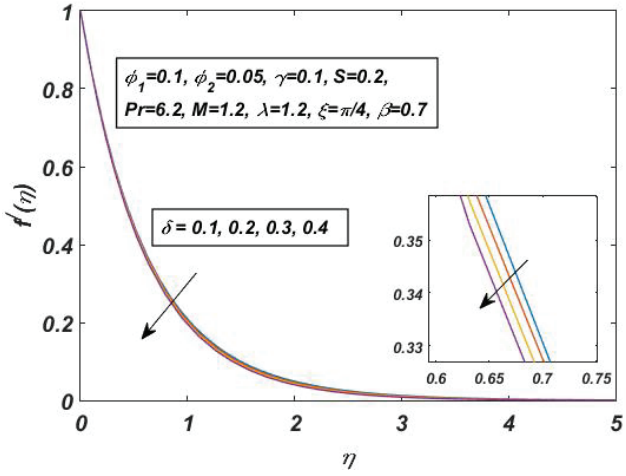

Figure 8. Impact of δ on velocity curve.

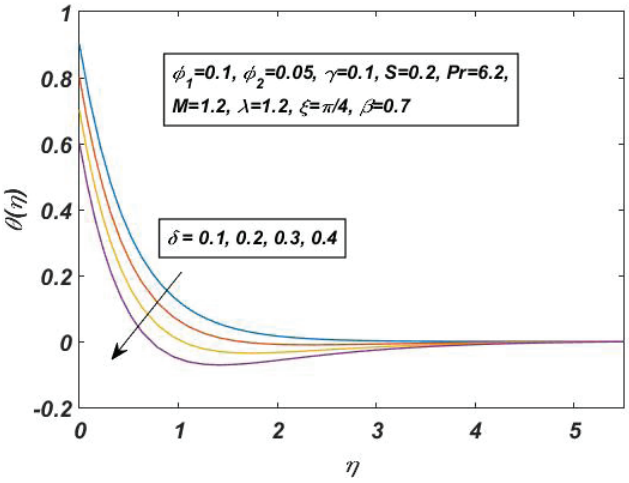

Figure 9. Impact of δ on thermal curve.

The flow speed and the thermal trend of the thermal stratification factor (δ) are portrayed in Figures 8 and 9. It is found that thermal stratification diminishes the boundary layer's velocity. The reason for this is that the convective potential between the heated wall and the surrounding fluid can be minimized due to heat stratification. Moreover, the force of resistance acts as a layering effect of heat stratification, helping to explain why the velocity is reducing. According to Figure 9, the thermal profile falls as thermal stratification increases. Strong thermal stratification leads to substantial variations in temperature between the various layers, which keep the lighter, warmer fluid at the top and the denser, cooler fluid at the bottom of the fluid. This stratified structure inhibits the fluid from mixing convectively, which prevents heat energy from being redistributed throughout the fluid volume. Simply, thermal stratification

Table 3. Calculated skin-friction and Nusselt number values for varying values of β, S, Pr, P, δ when $\phi_1 = 0.1$ and $\phi_2 = 0.05$

β	S	Pr	P	δ	Skin-Friction Coefficient	Nusselt Number
0.3	0.2	6.2	2	0.1	10.0195	2.7922
0.5					7.1166	2.7658
0.7					5.8678	2.7464
0.9					5.1718	2.7317
0.7	0.1	6.2	2	0.1	5.8787	2.9224
	0.2				5.8678	2.7464
	0.3				5.8516	2.5340
	0.4				5.7933	2.0799
0.7	0.2	0.7	2	0.1	5.6451	0.6674
		2			5.7178	1.2352
		6.2			5.8678	2.7464
		10			5.9263	3.7244
0.7	0.2	6.2	1	0.1	4.6634	2.9408
			2		5.8678	2.7464
			3		6.8673	2.5618
			4		7.7392	2.3673
0.7	0.2	6.2	2	0.1	5.8678	2.7464
				0.2	5.9199	2.7123
				0.3	5.9718	2.6768
				0.4	6.0234	2.6399

Table 4. Skin friction coefficient and Nusselt numbers for Casson-nanofluid and Casson-hybrid- nanofluid

		Cu/H_2O				Cu - MoS_2/H_2O		Change in %	
$\phi_1(MoS_2)$	$\phi_2(Cu)$	Skin Friction	Nusselt Number	$\phi_1(MoS_2)$	$\phi_2(Cu)$	Skin Friction	Nusselt Number	Skin Friction	Nusselt Number
0	0.01	3.9657	2.4929	0.1	0.01	5.2494	2.6591	32.37	6.66
	0.02	4.0847	2.5162		0.02	5.3970	2.6816	32.12	6.57
	0.03	4.2070	2.5393		0.03	5.5491	2.7036	31.90	6.47
	0.04	4.3329	2.5622		0.04	5.7060	2.7252	31.69	6.36
	0.05	4.4627	2.5849		0.05	5.8678	2.7464	31.48	6.24

reduces the thermal profile by restricting the fluid's ability to mix and homogenize its temperature. Moreover, as the fluid near the cylinder may be colder than the air that surrounds it, there is a negative temperature whenever there is sufficient thermal stratification. According to Deka and Paul [41], a strong stratification results in a reversal fluid flow over an infinite vertical cylinder. Moreover, in our investigation, we have found the same result for Cu/MoS_2 - H_2O Casson-hybrid-nanofluid flow.

Table 3 demonstrates how the physical non-dimensional factors β, S, Pr, P, δ influence the skin friction coefficient and Nusselt number. With increasing heat stratification factor, porosity parameter and Prandtl numbers, it is discovered that the absolute skin friction coefficient is elevated. This happens because the frictional effect caused by these parameters leads to a drop in the fluid's velocity. Paul et al. [49] demonstrated a diminution in the skin friction coefficient with the Casson factor for Cu - Al_2O_3/H_2O Casson hybrid nanofluid. However, in our investigation for Cu - MoS_2/H_2O Casson hybrid nano-fluid flow through a vertical cylinder, a declination in the absolute coefficient of skin friction is detected with the escalation of the variable of Casson fluid and the heat source. The heat transport rate is notably influenced by porous media. The numerical values of the Nusselt number diminish as the porosity parameter enhances. The findings for the heat source parameter, thermal stratification factor, and Casson fluid factor all exhibit the same pattern. i.e., as the thermal source, thermal stratification, and Casson fluid factors improve, the calculated findings of the Nusselt number decline. However, the Prandtl number exhibits the opposite trend from the Nusselt number. This illustrates that the values of the Nusselt index are boosted by the improved Prandtl number.

According to Table 4, the absolute skin friction and the Nusselt number are found to be improved with a boost in the volume proportion of Cu nanoparticles, maintaining ϕ_1 at zero. Additionally, it's been demonstrated that whenever the solid volume proportion of MoS_2 is estimated to be 0.1, the heat transfer rate jumps by more than 6.6%. It is manifest from the aforementioned results that hybrid Casson nanofluid has a thermal transmission rate that is significantly greater than that of Casson nanofluid. Furthermore, the Casson hybrid nanofluid increases absolute skin friction by nearly 32.3%.

CONCLUSION

This study investigated a thermally stratified Cu/MoS_2 - H_2O Hybrid Casson nanofluid flows over a vertically stretched cylinder in a permeable region while taking the heat source influence and inclined magnetic field into consideration. The study aims to investigate how the heat transfer rate changes when Cu - H_2O Casson nanofluid is modified to Cu - MoS_2 - H_2O Casson hybrid nanofluid in the existence of free convection and thermal stratification. Significant dimensionless elements and their impacts on thermal and velocity curves, friction drag, and heat transmission rate are investigated to ascertain whether physical variables influence the flow problem. The following is a list of the significant results from the current numerical study:

- The absolute value of the coefficient of skin friction is augmented for the non-dimensional parameters, Pr, δ and P, but for β and S the numerical findings of the absolute friction drag are diminished.
- The enhancing magnitudes of the Prandtl number (Pr) illustrate a rise in the rate of thermal transport.
- As the factorss β, P, S, and δ are boosted, it seems that the Nusselt number is decelerating.
- For a strong stratification results in a reversal fluid flow of Cu - MoS_2/H_2O Casson hybrid nanofluid.
- In contrast to the Casson nanofluid, the absolute friction of the Hybrid-casson nanofluid has increased by approximately 32.3%.
- The effective thermo transmission rate of Hybrid-casson nanofluid is boosted by up to 6.6% while contrasted to Casson nanofluid.

The findings of this study yield significant insights pertinent to the augmentation of heat transfer rates within bioengineering applications, particularly those involving fluid dynamics across vertically elongated cylinders situated within permeable regions. By comprehensively probing the behavior of hybrid nanofluids, exemplified by the Cu - MoS_2/H_2O composite, amidst various influential factors, this research underscores the potential for advancing heat

transfer efficiency across diverse systems, encompassing cooling apparatuses and energy conversion mechanisms. Furthermore, it elucidates a compelling trajectory for future investigations aimed at refining and optimizing hybrid nanofluids for heightened heat transfer efficacy. Subsequent research endeavors could encompass an expansive exploration of nanoparticle and base fluid permutations, alongside nuanced manipulations of thermal stratification levels and magnetic field orientations. Such endeavors aim to ascertain the optimal configurations tailored to specific application domains. Furthermore, the inquiry into additional parameters, including nanoparticle concentration and geometric variations, holds promise for further elucidating the intricacies governing heat transfer dynamics, thereby facilitating the design and implementation of markedly superior thermo transmission systems.

NOMENCLATURE

$(C_p)_f$, $(C_p)_{hnf}$	Specific thermo capacity of the fluid and hybrid nanofluid ($J\ kg^{-1}\ K^{-1}$)
$(C_p)_{s1}$, $(C_p)_{s2}$	Specific thermo capacity of MoS_2 and Cu ($J\ kg^{-1}\ K^{-1}$)
Gr_x	Grashof number
k_f, k_{bf}, k_{hnf}	Thermal conductivity of the fluid, nanofluid and hybrid nanofluid ($Wm^{-1}\ K^{-1}$)
k_{s1}, k_{s2}	Thermal conductivity of the solid nanoparticles ($Wm^{-1}\ K^{-1}$)
k	Permeability of porous media (m^2)
M	Magnetic parameter
P	Porosity factor
Pr	Prandtl Number
Re_x	Local Reynolds number
S	Heat source/sink parameter
T	Fluid temperature (K)
T_∞	Ambient fluid temperature (K)
T_w	Wall temperature (K)
u, v	The component of velocity along r and x directions (ms^{-1})
B_0	Strength of Magnetic field (NmA^{-1})
Q_0	Heat source/sink ($JK^{-1}\ m^{-3}\ s^{-1}$)

Greek symbols

β	Casson factor
ξ	Magnetic field Inclination
ψ	Stream function
$(\beta_T)_f$	Heat expansion of the fluid (K^{-1})
$(\beta_T)_{s1}$, $(\beta_T)_{s2}$	Heat expansion of the MoS_2 and Cu (K^{-1})
γ	The curvature parameter
δ	Thermal stratification factor
η	Similarity variable
λ	Thermal buoyancy factor
μ_f	Dynamic viscosity of the fluid (mPa)
μ_{hnf}	Hybrid nanofluid's dynamic viscosity (mPa)
σ_{hnf}	Hybrid nanofluid's electric conductivity ($Ohm^{-1}\ m^{-1}$)
ϕ_1,ϕ_2	Volume fractions of MoS_2 and Cu
ρ_f	Fluid density (kgm^{-3})
ρ_{hnf}	Hybrid nanofluid density (kgm^{-3})
ρ_{s1}	Density of MoS_2 (kgm^{-3})
ρ_{s2}	Density of Cu (kgm^{-3})

Subscripts

f	Fluid
b_f	Nanofluid
h_{nf}	Hybrid nanofluid
s	Solid

AUTHORSHIP CONTRIBUTIONS

All the authors equally contributed to this work.

DATA AVAILABILITY STATEMENT

The authors confirm that the data that supports the findings of this study are available within the article.

CONFLICT OF INTEREST

The author declared no potential conflicts of interest.

ETHICS

There are no ethical issues with the publication of this manuscript.

REFERENCE

[1] Choi SU, Eastman JA. Enhancing thermal conductivity of fluids with nanoparticles. Available at: https://ecotert.com/pdf/196525_From_unt-edu.pdf. Accessed Aug 7, 2024.

[2] Devi SA, Devi SS. Numerical investigation of hydromagnetic hybrid Cu-Al_2O_3/water nanofluid flow over a permeable stretching sheet with suction. Int J Nonlinear Sci Numer Simul 2016;17:249−257. [CrossRef]

[3] Devi SS, Devi SA. Numerical investigation of three-dimensional hybrid Cu-Al_2O_3/water nanofluid flow over a stretching sheet with effecting Lorentz force subject to Newtonian heating. Can J Phys 2016;94:490−496. [CrossRef]

[4] Ijaz Khan M, Hafeez MU, Hayat T, Imran Khan M, Alsaedi A. Magneto rotating flow of hybrid nanofluid with entropy generation. Comput Methods Programs Biomed 2020;183:105093. [CrossRef]

[5] Muneeshwaran M, Srinivasan G, Muthukumar P, Wang CC. Role of hybrid-nanofluid in heat transfer enhancement-A review. Int Commun Heat Mass Transf 2021;125:105341. [CrossRef]

[6] Sreenivasa BR, Faqeeh AJ, Alsaiari A, Alzahrani HA, Malik MY. Numerical study of heat transfer mechanism in the flow of ferromagnetic hybrid nanofluid over a stretching cylinder. Waves Random Complex Media 2022;14:1−17. [CrossRef]

[7] Yasir M, Malik ZU, Alzahrani AK, Khan M. Study of hybrid Al_2O_3-Cu nanomaterials on radiative flow over a stretching/shrinking cylinder: Comparative analysis. Ain Shams Engineer J 2023;14:102070. [CrossRef]
[8] Paul A, Nath JM, Das TK. Thermally stratified Cu-Al_2O_3/water hybrid nanofluid flow with the impact of an inclined magnetic field, viscous dissipation and heat source/sink across a vertically stretching cylinder. ZAMM-J. Appl Math Mech 2024;104:e202300084. [CrossRef]
[9] Ali A, Khan HS, Noor I, Pasha AA, Irshad K, Al Mesfer MK, et al. Hall effects and Cattaneo-Christov heat flux on MHD flow of hybrid nanofluid over a varying thickness stretching surface. Mod Phys Lett B 2024;38:2450130. [CrossRef]
[10] Saranya S, Al-Mdallal QM, Javed S. Shifted legendre collocation method for the solution of unsteady viscous-ohmic dissipative hybrid ferrofluid flow over a cylinder. Nanomater 2021;11:1512. [CrossRef]
[11] Saranya S, Baranyi L, Al-Mdallal QM. Free convection flow of hybrid ferrofluid past a heated spinning cone. Therm Sci Engineer Prog 2022;32:101335. [CrossRef]
[12] Saranya S, Duraihem FZ, Animasaun IL, Al-Mdallal QM. Quartic autocatalysis on horizontal surfaces with an asymmetric concentration: Water-based ternary-hybrid nanofluid carrying titania, copper, and alumina nanoparticles. Phys Scr 2023;98:075214. [CrossRef]
[13] Tarakaramu N, Sivakumar N, Tamam N, Satya Narayana PV, Ramalingam S. Theoretical analysis of Arrhenius activation energy on 3D MHD nanofluid flow with convective boundary condition. Mod Phys Lett B 2024;38:2341009. [CrossRef]
[14] Jagadeesh S, Chenna Krishna Reddy M, Tarakaramu N, Ahmad H, Askar S, Shukhratovich Abdullaev S. Convective heat and mass transfer rate on 3D Williamson nanofluid flow via linear stretching sheet with thermal radiation and heat absorption. Sci Rep 2023;13:9889. [CrossRef]
[15] Wang F, Tarakaramu N, Sivakumar N, Narayana PS, Babu DH, Ramalingam S. Three dimensional nanofluid motion with convective boundary condition in presents of nonlinear thermal radiation via stretching sheet. J Indian Chem Soc 2023;100:100887. [CrossRef]
[16] Tarakaramu N, Satya Narayana PV, Sivakumar N, Harish Babu D, Bhagya Lakshmi K. Convective conditions on 3D magnetohydrodynamic (MHD) non-Newtonian nanofluid flow with nonlinear thermal radiation and heat absorption: A numerical analysis. J Nanofluids 2023;12:448−457. [CrossRef]
[17] Devi MR, Sivakumar N, Tarakaramu N, Narayana PV. The impact of heat source and thermal radiation on nano-bioconvection containing gyrotactic microorganism flow in parallel channel. AIP Conf Proc 2023;2852:050010. [CrossRef]
[18] Hussain S, Ali A, Rasheed K, Pasha AA, Algarni S, Alqahtani T, et al. Application of response surface methodology to optimize MHD nanofluid flow over a rotating disk with thermal radiation and joule heating. Case Stud Therm Engineer 2023;52:103715. [CrossRef]
[19] Gari AA, Islam N, Bibi S, Majeed A, Ali K, Jamshed W, et al. A thermal case study of three dimensional MHD rotating flow comprising of multi-wall carbon nanotubes (MWCNTs) for sustainable energy systems. Case Stud Therm Engineer 2023;50:103504. [CrossRef]
[20] Ali A, Kanwal T, Awais M, Shah Z, Kumam P, Thounthong P. Impact of thermal radiation and non-uniform heat flux on MHD hybrid nanofluid along a stretching cylinder. Sci Rep 2021;11:20262. [CrossRef]
[21] Khan U, Zaib A, Ishak A, Sherif ES, Waini I, Chu YM, et al. Radiative mixed convective flow induced by hybrid nanofluid over a porous vertical cylinder in a porous media with irregular heat sink/source. Case Stud Therm Engineer 2022;30:101711. [CrossRef]
[22] Khan Z, Jan R, Jawad M, Hussain F. Radiation heat transfer of hybrid nanofluid stagnation point flow across a stretching porous cylinder. Therm Sci Engineer 2023;6:2595. [CrossRef]
[23] Suresha R, Arunkumar R, Hanumagowda BN, Abduvalieva D, Tarakaramu N, Awwad FA, et al. Combined effect of magneto hydrodynamics, couple stress, and viscosity variation on squeeze film characteristics of a cylinder and rough flat plate. SN Appl Sci 2023;5:350. [CrossRef]
[24] Casson N. Flow equation for pigment-oil suspensions of the printing ink-type. In: Mill CC, editor. Rheology of Disperse Systems. Oxford: Pergamon Press; 1959. pp. 84−104.
[25] Kamran A, Hussain S, Sagheer M, Akmal N. A numerical study of magnetohydrodynamics flow in Casson nanofluid combined with Joule heating and slip boundary conditions. Results Phys 2017;7:3037−3048. [CrossRef]
[26] Ramesh GK, Kumar KG, Shehzad SA, Gireesha BJ. Enhancement of radiation on hydromagnetic Casson fluid flow towards a stretched cylinder with suspension of liquid-particles. Can J Phys 2018;96:18−24. [CrossRef]
[27] Naqvi SM, Muhammad T, Asma M. Hydromagnetic flow of Casson nanofluid over a porous stretching cylinder with Newtonian heat and mass conditions. Phys A Stat Mech Appl 2020;550:123988. [CrossRef]
[28] Ragupathi P, Saranya S, Mittal HV, Al-Mdallal QM. Computational study on three-dimensional convective Casson nanofluid flow past a stretching sheet with Arrhenius activation energy and exponential heat source effects. Complexity 2021;2021:1−16. [CrossRef]

[29] Krishna MV, Ahammad NA, Chamkha AJ. Radiative MHD flow of Casson hybrid nanofluid over an infinite exponentially accelerated vertical porous surface. Case Stud Therm Engineer 2021;27:101229. [CrossRef]

[30] Jyothi AM, Varun Kumar RS, Madhukesh JK, Prasannakumara BC, Ramesh GK. Squeezing flow of Casson hybrid nanofluid between parallel plates with a heat source or sink and thermophoretic particle deposition. Heat Transf 2021;50:7139−7156. [CrossRef]

[31] Zeeshan A, Mehmood OU, Mabood F, Alzahrani F. Numerical analysis of hydromagnetic transport of Casson nanofluid over permeable linearly stretched cylinder with Arrhenius activation energy. Int Comm Heat Mass Transf 2022;130:105736. [CrossRef]

[32] Wang F, Zhang J, Algarni S, Naveed Khan M, Alqahtani T, Ahmad S. Numerical simulation of hybrid Casson nanofluid flow by the influence of magnetic dipole and gyrotactic microorganism. Waves Rand Complex Med 2022:1−16. [CrossRef]

[33] Saranya S, Al-Mdallal QM, Animasaun IL. Shifted Legendre collocation analysis of time-dependent Casson fluids and Carreau fluids conveying tiny particles and gyrotactic microorganisms: Dynamics on static and moving surfaces. Arab J Sci Engineer 2023;48:3133−3155. [CrossRef]

[34] Tarakaramu N, Reddappa B, Radha G, Abduvalieva D, Sivakumar N, Awwad FA, et al. Thermal radiation and heat generation on three-dimensional Casson fluid motion via porous stretching surface with variable thermal conductivity. Open Phys 2023;21:20230137. [CrossRef]

[35] Wang F, Tarakaramu N, Govindaraju MV, Sivakumar N, Lakshmi KB, Narayana PS, et al. Activation energy on three-dimensional Casson nanofluid motion via stretching sheet: Implementation of Buongiorno's model. J Indian Chem Soc 2023;100:100886. [CrossRef]

[36] Radha G, Reddappa B, Tarakaramu N, Srinivas VS, Ramalingam S, Reddy NM, et al. Three dimensional casson nanofluid flow with convective boundary layer via stretching sheet. J Adv Zool 2023;44:1121−1129.

[37] Shah Z, Raja MA, Khan WA, Shoaib M, Tirth V, Algahtani A, et al. Computational intelligence paradigm with Levenberg-Marquardt networks for dynamics of Reynolds nanofluid model for Casson fluid flow. Tribol Int 2024;191:109180. [CrossRef]

[38] Masthanaiah Y, Tarakaramu N, Khan MI, Rushikesava A, Moussa SB, Fadhl BM, et al. Impact of viscous dissipation and entropy generation on cold liquid via channel with porous medium by analytical analysis. Case Stud Therm Engineer 2023;47:103059. [CrossRef]

[39] Ishak A, Nazar R, Pop I. Mixed convection boundary layer flow adjacent to a vertical surface embedded in a stable stratified medium. Int J Heat Mass Transf 2008;51:3693−3695. [CrossRef]

[40] Mukhopadhyay S, Mondal IC, Gorla RS. Effects of thermal stratification on flow and heat transfer past a porous vertical stretching surface. Heat Mass Transf 2012;48:915−921. [CrossRef]

[41] Deka RK, Paul A. Transient free convection flow past an infinite moving vertical cylinder in a stably stratified fluid. J Heat Transf 2012;134:0425031. [CrossRef]

[42] Deka RK, Paul A. Transient free convection flow past an infinite vertical cylinder with thermal stratification. J Mech Sci Technol 2012;26:2229−2237. [CrossRef]

[43] Deka RK, Paul A. Convectively driven flow past an infinite moving vertical cylinder with thermal and mass stratification. Pramana 2013;81:641−665. [CrossRef]

[44] Paul A, Deka RK. Unsteady natural convection flow past an infinite cylinder with thermal and mass stratification. Int J Engineer Math 2017;2017:8410691. [CrossRef]

[45] Khashi'ie NS, Arifin NM, Hafidzuddin EH, Wahi N. Thermally stratified flow of Cu-Al_2O_3/water hybrid nanofluid past a permeable stretching/shrinking circular cylinder. J Adv Res Fluid Mech Therm Sci 2019;63:154−163.

[46] Jafar MA, Abbas Z, Hasnain J. Thermally stratified radiative flow of non-Newtonian fluid between two discs executing diverse type of in-plane motion. Case Stud Therm Engineer 2021;26:101187. [CrossRef]

[47] Ahmad S, Naveed Khan M, Rehman A, Felemban BF, Alqurashi MS, Alharbi FM, et al. Analysis of heat and mass transfer features of hybrid Casson nanofluid flow with the magnetic dipole past a stretched cylinder. Appl Sci 2021;11:11203. [CrossRef]

[48] Alkasasbeh H. Numerical solution of heat transfer flow of casson hybrid nanofluid over vertical stretching sheet with magnetic field effect. CFD Lett 2022;14:39−52. [CrossRef]

[49] Paul A, Das TK, Nath JM. Numerical investigation on the thermal transportation of MHD Cu/Al_2O_3-H_2O Casson-hybrid-nanofluid flow across an exponentially stretching cylinder incorporating heat source. Phys Scr 2022;97:085701. [CrossRef]

[50] Shampine LF, Kierzenka J, Reichelt MW. Solving boundary value problems for ordinary differential equations in MATLAB with bvp4c. Tutor Notes 2000;2000:1−27.

[51] Paul A, Nath JM, Das TK. An investigation of the MHD Cu-Al_2O_3/H_2O hybrid-nanofluid in a porous medium across a vertically stretching cylinder incorporating thermal stratification impact. J Ther Engineer 2023;9:799−810. [CrossRef]

[52] Ghadikolaei SS, Gholinia M, Hoseini ME, Ganji DD. Natural convection MHD flow due to MoS_2-Ag nanoparticles suspended in $C_2H_6O_2H_2O$ hybrid base fluid with thermal radiation. J Taiwan Inst Chem Engineer 2019;97:12−23. [CrossRef]

[53] Elbashbeshy EM, Emam TG, El-Azab MS, Abdelgaber KM. Laminar boundary layer flow along a stretching cylinder embedded in a porous medium. Int J Phys Sci 2012;7:3067−3072. [CrossRef]